A novel 1,1′-bis[4-(5,6-dimethyl-1*H*-benzimidazole-1-yl)butyl]-4,4′-bipyridinium dibromide (viologen) for a high contrast electrochromic device

Rambabu Sydam[a], Melepurath Deepa[a,*], Amish G. Joshi[b]

[a]Department of Chemistry, Ordnance Factory Estate, Indian Institute of Technology Hyderabad, Yeddumailaram-502205, Andhra Pradesh, India

[b]National Physical Laboratory, Dr. K.S. Krishnan road, New Delhi-110012, India

Abstract

A new electrochromic viologen, 1,1′-bis-[4-(5,6-dimethyl-1H-benzimidazole-1-yl)-butyl]-4,4′-bipyridinium dibromide (IBV) was synthesized by di-quaternization of 4,4′-bipyridyl using 1-(4-bromobutyl)-5,6-dimethyl-1H-benzimidazole. X-ray photoelectron spectroscopy confirmed the formation of the IBV (viologen) salt as distinct signals due to quaternary nitrogen and neutral nitrogen, and ionic-bonded bromide were identified. An electrochromic device encompassing a dicyanamide ionic liquid based gel polymeric electrolyte with high ionic conductivity, a thermal decomposition temperature above 200 ^{o}C, and a stable voltage window of ~4 V with the IBV viologen dissolved therein, was constructed. IBV is a cathodically coloring organic electrochrome and the device underwent reversible transitions between transparent and deep blue hues; the color change was accompanied by an excellent optical contrast (30.5 % at 605 nm), a remarkably high coloration efficiency of 725 cm^2 C^{-1} at 605 nm and switching times of 2-3 s. Electrochemical impedance spectroscopy revealed an unusually low charge transfer resistance at the IBV salt/gel interface, which

promotes charge propagation and is responsible for the intense coloration of the reduced radical cation state. The device was subjected to repetitive switching between the colored and bleached states and was found to incur almost no loss in redox activity, upto 1000 cycles, thus ratifying its suitability for electrochromic window/display applications.

KEYWORDS *: Viologen, electrochromic device, Prussian blue, dicyanamide ionic liquid*

1. Introduction

Viologens are di-quaternized salts of 4,4′-bipyridyl and they undergo a significant change in their visible extinction coefficient upon reduction to radical cations [1,2]. This visual transformation from an optically transparent hue to an intense colored hue, can be triggered by light irradiation or by a chemical reductant or by application of an electric current or voltage. The change in color of viologens induced by an electric field, has been of tremendous utilitarian value, as viologens are incorporated in electrochromic devices (ECDs) and they find applications in smart windows, glare reduction mirrors and high contrast displays [3-5]. The type-II viologen salts are solution-phase compounds and therefore, typically they are dissolved in the electrolyte [6] for use in an electrochromic device (ECD). Viologens in electrolyte solution exist in the dicationic form and unless charge transfer interactions with the anions are present, they are generally colorless [7]. In an electrochromic device, they are reduced to colored radical cations, at the cathode, by an electrochemical reaction. The colored radical cation is insoluble in the electrolyte and appears in the form of a colored layer over the transparent conducting electrode surface. They easily revert to the soluble and colorless dicationic form, by reversing the applied potential [6]. Hence, this reversible, redox capability accompanied by a simultaneous color contrast renders viologens as frontrunners for cathodic electrochromes.

In the past, there have been several reports devoted to the use of 4,4′-bipyridine derivatives in electrochromic device [6,8,9]. Mortimer *et al*. reported a very high contrast and fast optical switching for a color-reinforcing electrochromic device composed of a novel ruthenium purple chromophore as anode and the di-methyl viologen as the cathodic colorant [10]. In another study, a surface confined phosphonoethyl viologen modified mesoporous nanocrystalline titania electrode was found to display rapid color-bleach kinetics of the order of 1-2 s, alongwith a high optical density change of 1.2 [11], thus proving to be an ideal candidate for large contrast displays. In yet another study, an electrochromic cell

containing a layer-by-layer assembly of silsesquioxane nanoparticles incorporating a polymeric viologen showed a transmission modulation of 50 % and a coloration efficiency of 205 cm^2 C^{-1} at 550 nm, which validated its use for electrochromic displays [12]. An all-solid-state electrochromic device with 2,2,6,6-tetramethyl-1-piperidinyloxy (TEMPO) and heptyl viologen showed a coloration efficiency above 300 cm^2 C^{-1} in the visible region [13]. In a recent report, a fast switching and high contrast electrochromic device based on viologen and Prussian blue (PB)/antimony tin oxide nano-composites showed a large coloration efficiency exceeding 912 cm^2 C^{-1} [14]. Cycling stability measurements revealed an operational endurance of about 4000 cycles for an ECD based on Polybutyl viologen (PBV) and PB with a solid-state succinonitrile -based electrolyte [3]. Notably, an electrochromic composite prepared by a layer-by-layer (LBL) assembly of poly(hexyl viologen) (PXV) and poly(3,4-ethylenedioxythiophene):poly(styrene sulfonate), exhibited a maximum transmittance change of 82.1% at 525 nm [15].

Although conventional N,N′-dimethyl- or N,N′-diheptyl-4,4′-bipyridinium salts and their modified forms have been exhaustively reconnoitered for electrochromic applications [16], and have been fairly successful, even commercially [17,18], nonetheless very high optical contrast (> 40 %), ultra high coloration efficiencies (> 300 cm^2 C^{-1}) in the visible region and fast switching between colored and bleached states (~1-2 s, for areas greater than 2 cm^2), are very much desirable for both reflective and transmissive electrochromic devices. The need for developing new viologens stems from the fact that traditional viologens like di-heptyl viologen are planar molecules, and when reduced to radical cations, they re-arrange themselves on the electrode surface to form a stack like assembly, wherein each molecule lies directly above the other. Such a compact structure is resistive to oxidation and within a few cycles, the redox process becomes irreversible and the device acquires a permanently colored state. To circumvent this, bulky substituents are attached to the N,N′- positions of the bipyridyl, which coerce the radical cation out of planarity, prevent re-arrangement, thus inhibit stacking and make the process reversible and therefore rendering them conducive for switchable electrochromic devices [19-21]. To

address these issues, we synthesized a new viologen, which showed an extremely high contrast, good color uniformity, fast response time and an extraordinarily high coloration efficiency, significantly improved in comparison to reported values for viologens. A novel derivative of viologen salt containing the 5,6-dimethylbenzimidazole moiety connected by a butyl chain was synthesized and characterized. For practical applications, an anodically coloring complementary moiety is also employed in the electrochromic devices, to enhance contrast ratio. Prussian blue films are widely used as anodic electrochromes as they undergo reversible change from Prussian white (transparent) to Prussian blue upon oxidation and also offer charge balancing feature, the latter being beneficial for long-term cycling stability [3,22,23]. We used a gel polymeric electrolyte, for fabricating an electrochromic device. The gel was based on an ionic liquid namely, 1-ethyl-3-methylimidazolium dicyanamide and the electrochromic viologen salt: 1,1′-bis[4-(5,6-dimethyl-1H-benzimidazole-1-yl)butyl]-4,4′-bipyridinium dibromide (IBV) was dissolved therein.

We used an *in-situ* thermal polymerization technique for solidifying the liquid electrolyte, with 2-hydroxyethyl methacrylate as the monomer, as we found in a previous study that this method leads to devices with good interfacial contacts, which effectively translates into fast switching [24]. High ionic conductivity, good thermal stability and a wide electrochemical potential stability window for the semi-solid gel electrolyte, characteristics which are quintessential for any practical application, were ensured by the use of the dicyanamide ionic liquid. The successful formation of the viologen was ascertained by X-ray photoelectron spectroscopy (XPS), and the electrochemical response and coloration of the viologen based electrochromic device was followed by cyclic voltammetry, spectroelectrochemistry, and electrochemical impedance spectroscopy. The performance attributes of the viologen based electrochromic device coupled with the ease of synthesis of a stable polymeric electrolyte and facile device fabrication, serve as a paradigm for developing enhanced contrast, durable and rapid switching electrochromic devices for display and smart window applications.

2. Experimental

2.1 Materials

4,4′-bipyridyl, 5,6-dimethyl-1H-benzimidazole, 2-hydroxyethyl methacrylate (HEMA), 1,4-dibromobutane were procured from Sigma Aldrich. Potassium ferricyanide ($K_3[Fe(CN)_6]$), iron(III)chloride ($FeCl_3$), K_2CO_3, acetonitrile, N,N-dimethylformamide, 1-ethyl-3-methylimidazolium dicyanamide ($EtMeIm^+N(CN)_2^-$), benzoylperoxide (25% H_2O), hydrochloric acid (35% HCl), ethyl acetate, petroleum ether, acetone, n-hexane, diethyl ether, dichloromethane and methanol were procured from Merck. Ultrapure water (resistivity 18.2 MΩ cm) obtained through the Millipore Direct-Q 3 UV system was used as the solvent. Fluorine doped tin oxide (SnO2:F or FTO) coated glass substrates were purchased from Pilkington (sheet resistance: 14 Ω sq^{-1}) and used after cleaning with 10 % HCl, soap solution and distilled water and acetone.

2.2 Synthesis of 1-(4-bromobutyl)-5,6-dimethyl-1H-benzimidazole (**2**)

To 1.0 g of 5,6-dimethyl-1H-benzimidazole(**1**) (6.8 mmol), 1.4 g of K_2CO_3 (10.2 mmol) was added and dissolved in 30 mL of dried acetonitrile and stirred for 30 minutes under ice cold conditions. 1.77 g of 1,4-dibromobutane (8.2 mmol) was added drop-wise under N_2 atmosphere and the reaction was stirred at 60 ^{0}C for 6-8 h. The reaction mixture was filtered and the filtrate was concentrated under reduced pressure. Crude product was purified through the column chromatography (dichloromethane/ethyl acetate**:** 95:5 to 85:15) as pale yellow viscous liquid(**2)**. Yield (0.86 g, 45%) for (**2**). This compound is unstable and the next reaction was implemented immediately. [TLC control (dichloromethane/ethyl acetate 7:3, R_f(**1**) = 0.50, R_f (**2**)=0.60, UV detection]. IR (MIR-ATR, 4000–600 cm^{-1}): ν_{max} = 3075, 2923, 2853, 1627, 1563, 1498, 1469, 1218, 1142, 1022, 870, 841, 720,621 cm^{-1}. ^{1}H NMR ($CDCl_3$, 400 MHz): δ = 7.76 (s, 1H, Ar-H), 7.55 (s, 1H, Ar-H), 7.15 (s, 1H, Ar-H), 4.13–4.17 (t, 2H, -CH_2), 3.36–3.40 (t, 2H, -CH_2), 2.37 (s, 3H, Ar-CH_3), 2.39 (s, 3H, ArCH_3), 2.00-2.05 (m, 2H,-CH_2) and 1.84-1.89 (m,2H,-

CH_2) ppm. ^{13}C NMR ($CDCl_3$, 100 MHz): δ=142.5 (s, Ar-C), 142.0 (d, Ar-C), 132.2 (s, 2C, Ar-C), 131.1 (s, Ar-C), 120.4 (d, Ar-CH), 109.7 (d, Ar-CH), 44.2 (t, -CH_2), 32.6 (t, -CH_2), 29.7 (t, -CH_2), 28.4 (t, -CH_2) and 20.6 (q, Ar-CH_3), 20.3 (q, Ar-CH_3) ppm. HR-MS (APCI+) m/z calculated for $[C_{13}H_{18}BrN_2]^+ = [(M+H)]^+$: 281.0648; found: 281.0640.

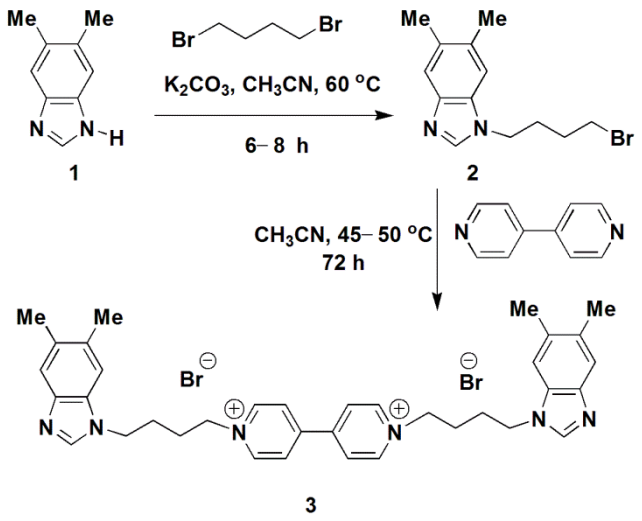

Scheme 1: Two step synthesis of IBV salt

Synthesis of 1,1′-bis[4-(5,6-dimethyl-1H-benzimidazole-1-yl)butyl]-4,4′-bipyridinium dibromide (IBV) (**3**)

To 1.0 g of 1-(4-bromobutyl)-5,6-dimethyl-1H-benzimidazole (**2**) (3.56 mmol), added 0.221 g of 4,4′-bipyridyl (1.42 mmol), dissolved in dried acetonitrile (50 mL) and continued stirring under N_2 atmosphere at 45-50 ^{0}C for 72 h. The crude precipitate was washed with ethyl acetate to remove unreacted 4,4′-bipyridyl. The precipitate was purified by repeated precipitation using methanol/acetone. The product was washed with n-hexane and with dry diethyl ether, and vacuum dried at 60 ^{0}C for 4 h. This viologen salt (**3**) (IBV) is a pale yellow powder. Yield (0.845 g, 83%) and it was calculated with respect to 4,4′-bipyridyl.

Melting point: Decomposed at 170 ^{0}C

IR (MIR-ATR, 4000–600 cm^{-1}): ν_{max} = 3018, 2980, 2944, 1637, 1563, 1488, 1447, 1362, 1218, 1175, 1022, 1001, 864, 817, 720, 603 cm^{-1}. ^{1}H NMR : (CD_3OD, 400 MHz): δ=9.06-9.09 (dd, 2H, Ar-H), 8.92-8.93 (d, 1H, Ar-H), 8.70-8.74 (m, 2H, Ar-H), 8.33-8.42 (m, 2H, Ar-H) 7.97 (d, 1H, Ar-H), 7.86-7.89 (m, 2H, Ar-H), 7.45-7.49 (t, 1H, Ar-H), 7.23-7.27 (m, 2H, Ar-H), 7.15 (d, 1H, Ar-H) ppm. ^{13}C NMR (CD_3OD, 100 MHz): δ=151.8 (d, 2C Ar-CH), 151.2 (s, 2C, Ar-C), 138.7 (d, 2C, Ar-CH), 131.4 (d, 2C, Ar-CH), 127.2 (s, 2C, Ar-C), 127.0 (d, 2C, Ar-CH), 123.6 (d, 2C, Ar-CH), 123.5 (s, 2C, Ar-C), 123.2 (s, 2C, Ar-C), 120.2 (d, 2C, Ar-CH), 114.1 (s, 2C, Ar-C), 111.5 (d, 2C, Ar-CH), 47.6 (t, 2C, N-CH_2), 45.3 (t, 2C, N-CH_2), 27.1 (t, 2C, N-CH_2-CH_2), 26.8 (t, 2C, -CH_2-CH_2-N) and 20.5 (q, 4C, 4×Ar-CH_3) ppm. HR-MS (ESI+) m/z calculated for $[C_{36}H_{42}Br_2N_6]^+$ = $[M+2Na]^+$: 762.2; found: 762.2.

2.3 Fabrication of electrochromic device with IBV salt

The monomer HEMA was passed through a neutral alumina column to remove the inhibitor. The ionic liquid and N,N-dimethylformamide were taken in a 1:2 weight ratio, and 20-25 wt% of HEMA and 3-4 wt % of benzoyl peroxide were added. For preparing an electrochromic device, 0.025 M IBV salt was dissolved in the electrolyte solution. All the contents were sonicated for 15 minutes. Prussian blue films were grown from a solution of 10 mM $K_3[Fe(CN)_6]$ and 10 mM $FeCl_3$ in 0.01 N HCl in a three electrode cell, using Ag/AgCl/KCl as reference electrode by applying a fixed potential of +1.5 V for 300 s to a SnO_2:F coated glass substrate. Films were washed in a solution of 0.01 N HCl and deionized water mixed in a 2:3 volume ratio and stored in air. A cavity was created between two electrodes; cathode was a blank FTO coated glass substrate and the anode was a Prussian blue film coated on FTO/glass. A 0.64 mm thick and 3 mm wide adhesive acrylic tape was employed as the spacer, which prevented the shorting of the two electrodes and also held the device assembly together. More details about device fabrication can be found in our previous report [24]. The electrolyte solution containing the monomer (HEMA) and the IBV salt was injected into the device. The *in-situ* thermal polymerization of the monomer was carried out by heating the above prepared electrolyte solution at 60 ^0C for 12 – 15 h in an

oven. A transparent, pale blue colored device encompassing the electrolyte in the form of a gel was obtained and all the edges were sealed with epoxy. The device, hereafter is referred to as the IBV/P(HEMA)/EtMeIm^{+}N(CN)$_2^{-}$/PB device.

2.4 Instrumentation techniques

X-ray photoelectron spectroscopy (XPS) was carried out on a Perkin Elmer 1257 model operating at a base pressure of ~4.2 × 10^{-8} Torr (100 Watt, 15 KV) with a non-monochromatized Mg Kα line at 1253.6 eV, an analyzer pass energy of 60 eV, and a hemispherical sector analyzer capable of 25 meV resolution. The overall instrumental resolution was about 0.3 eV. The core level spectra were deconvoluted using a non-linear iterative least squares Gaussian fitting procedure. For all fitting multiplets, the FWHMs were fixed accordingly. Corrections due to charging effects were taken care of by using C(1s) as an internal reference and the Fermi edge of a gold sample. Jandel Peak FitTM (version 4.01) program was used for the analyses. Thermogravimetric analysis (TGA, TA instruments, Q600) were carried out for in-situ polymerized gel electrolyte (semi-solid), IL (liquid) and IBV salt (solid powder) from 30 – 600 ^{0}C temperature with 10 ^{0}C/minute ramp rate under N2 atmosphere. Cyclic voltammetry (CV) for the devices and linear sweep voltammetry (LSV) for the electrolyte gel were performed on an Autolab PGSTAT 302N Potentiostat/Galvanostat coupled with a NOVA 1.7 software. The optical density and transmittance of the device was measured *in-situ*, on a Shimadzu UV-Visible-NIR 3600 spectrophotometer under dc potentials of different magnitudes (applied for a 60 s duration). Electrochromic switching response of the device was performed under a square wave potential, at a fixed monochromatic wavelength, using the same spectrophotometer, in kinetic mode. Electrochemical impedance spectroscopy was also performed for the device, on Autolab; an ac voltage of 10 mV was superimposed over different dc potentials. Z″ *versus* Z′ plots were obtained over a frequency range of 10^{6} Hz to 0.1 Hz. Ionic conductivity (σ) of the electrolyte gel was determined by sandwiching the gel

between two Pt electrodes and measuring impedance under a zero dc bias and 10 mV ac voltage at different temperatures in a controlled temperature bath. The point of inception of the Z″ *versus* Z′, yielded the bulk electrolyte resistance (R_s) and conductivity was calculated using $\sigma = 1/R_s$ (d/a), where d is the distance between the two Pt electrodes and a is the area of the electrode.

3. Results and discussion

3.1 XPS studies

The survey spectrum of the IBV salt and the core level spectra are shown in Figure 1. The survey spectrum shows distinct peaks from C1s, Br3p, Br3d, N1s and O1s, indicating the presence of these elements in the sample. The deconvoluted C1s spectrum shows two peaks at 284.5 and 285.8 eV, which are attributed to the C-C and C-N groups in the salt. The deconvoluted N1s spectrum shows three peaks at 403.4, 401.1 and 396.3 eV, which can be attributed to the quaternary nitrogen ($-N^+$), and, the –N= bonds and the tertiary nitrogen groups respectively. The Br3d core level spectrum shows an intense, symmetric peak centered at 67 eV, which is slightly downshifted in comparison to the Br3d peak typically observed at 70 eV for covalently bonded bromine [25-27]. This shift to lower binding energy is suggestive of ionic Br^-, implying the formation of N^+-Br^- ionic bonds or salt formation. Similarly, an enlarged view of the two components of the Br3p spin-orbit split doublet is shown as an inset of Figure 1a. The peaks at 180 and 187 eV with an almost 2:1 intensity ratio, are ascribed to the Br3p3/2 and Br3p1/2 components. Since these two peaks appear at positions, downshifted relative to the positions of 183 and 190 eV for covalently bonded Br in literature [25]; this implies that the nature of the bond formed by Br in the IBV salt is ionic and not covalent. The lack of evidence for the existence of covalently bonded Br, also indicates that the final product (or IBV salt) contains no traces of unreacted precursor (containing covalently bound Br). Thus, XPS data analysis provides evidences in support of the formation of the IBV salt as proposed in scheme 1.

3.2 Electrolyte and IBV salt characteristics

TGA plots of the in-situ polymerized gel electrolyte (semi-solid), IL (ionic liquid) and IBV salt (solid powder) in the 30–600 ^{0}C temperature range are shown in Figure 2a and 3 (3 is the TGA plot of the IBV solid). The figure shows the weight losses in the samples as a function of temperature. For in-situ gel, the initial weight loss upto 60 ^{o}C is attributed to the evaporation of adsorbed moisture from the sample; thereafter, a plateau was observed till 270 ^{o}C, indicating that the gel undergoes decomposition only at high temperatures and therefore can be incorporated in an electrochromic device (for which usually the upper limit of operational temperature is stipulated to be ~ 90 ^{o}C). The pristine ionic liquid was found to be stable upto 290 ^{0}C. The IBV salt decomposed only at ~270 ^{0}C (Figure 3), which illustrates its' suitability for any electrochemical device application. The photographs of the electrolyte solution (prior to temperature induced polymerization) with and without the IBV salt are shown as insets in Figure 3. The IBV salt completely dissolves in the liquid electrolyte to yield a yellow transparent solution, indicating good compatibility with organic solvents like DMF and the ionic liquid. The ability of the IBV salt to form radical cations by chemical reduction was also confirmed by using sodium hydrosulfite in ammonia, and a deep blue color was obtained in solution phase (Figure 3, inset c). The linear sweep voltammogram of the in-situ polymerized gel is shown in Figure 2b, and the gel was observed to be electrochemically inert in the voltage range of –2 V to +2 V, indicating a potential stability window of about ~4 V, which is adequate for electrochromic device application. The transmittance of the gel electrolyte in the visible region (Figure 2c) was found to vary between 60-65 %. Since the electrolyte is optically transparent in the 400-750 nm wavelength region, it can be employed for fabricating transmissive electrochromic devices. The ionic conductivity of the gel electrolyte was found to be 0.26 mS cm^{-1} at room temperature and it varied insignificantly with temperature; as conductivity increased from 0.21 to 0.27 mS cm^{-1} on raising temperature from -5 and 10 to 70 ^{o}C in steps of 10 ^{o}C (Figure 2d). Previously, electrochromic devices employing methacrylate-based polymer electrolytes exhibited good ionic conductivity of 0.7 mS cm^{-1} at 20 ^{0}C, which is comparable to our observed value.[28] For any

electrochemical device, ideally, the ionic conduction capability of the electrolyte should be invariant within the operational temperature window of the device. The in-situ polymerized gel fulfills this pre-requisite, thereby justifying its' use as the electrolyte in a solid-state electrochromic device.

3.3 Cyclic voltammetry

"Type II" electrochromes, undergo a soluble to insoluble transition on electrochemical reduction from aqueous solutions [1]. Similarly, the IBV salt prepared herein is a "type II" electrochrome. The cyclic voltammograms for the IBV/P(HEMA)/EtMeIm^{+}N(CN)$_2^{-}$/PB device, recorded within potential limits of –0.8 to +0.2 V and between –1.5 to +0.2 V are shown in Figure 4a and b. In the cathodic branch, the reduction peak observed at –0.62 V (Figure 4a) is assigned to the formation of the dark blue radical cation salt on the FTO surface, which is followed by oxidation to the di-cation and its dissolution in the electrolyte at -0.53 V, in the reverse sweep. The peak separation was 0.09 V. The one electron oxidation and reduction reaction occurs as shown in the first step of equation (1).

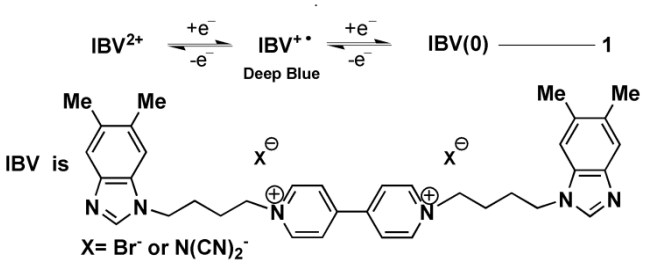

The cyclic voltammogram shown in Figure 4b illustrates the two redox states of the IBV salt. We observed a second reduction peak at –1.08 V. These two peaks correspond to monovalent radical cation formation followed by formation of the neutral viologen, upon further increasing the reduction potential, as shown in the second step of equation (1). In the anodic branch, the first oxidation peak at –1.06 V corresponds to radical cation formation and the second peak at –0.65 V is attributed to the di-cation formation. The neutral viologen is colorless or is expected to have a pale color. However, we did not

observe any pale colored deposit on the electrode in the cathodic branch, thus providing evidence for comproportionation reaction. Also, the ratio of peak currents represented by i_{pc}/i_{pa} is 1.6 for the first pair of redox peaks and it is considerably skewed for the second pair of redox peaks. The fact that it is very much greater than unity for the second pair of redox peaks indicates that a comproportionation reaction, as shown in equation (2), involving the fully oxidized di-cation and the fully reduced neutral viologen occurs at the electrode surface at higher potentials [29,30].

$$IBV^{2+} + IBV(0) \rightarrow 2IBV^{+\bullet} \qquad (2)$$

The dimer formation is generally not feasible in non-aqueous solvents [13,31]. However, in a previous study, Sammells *et al.* observed a deep violet color as the product of mono-reduction of a heptyl viologen, and a more intense violet color (of the same hue) was the product of di-reduction [32]. Here, we too observed the deep blue hue for IBV/P(HEMA)/$EtMeIm^{+}N(CN)_2^{-}$/PB device, even when the negative bias was increased to –2.6 V, indicating that the neutral viologen exists probably as a transition state entity.

Since the reversible transition between the deep blue and colorless hues was easily achieved within the voltage limits of –0.8 to +0.2 V, the effect of scan rate on the redox response of the IBV salt was examined within these limits (Figure 4c). With increasing scan rate (from 2 to 100 mV s^{-1}) , the oxidation peak shifts to less negative potentials, the reduction peak shifts to more negative potentials, and the peak separation increases.

3.4 Spectroelectrochemistry of IBV based device

The in-situ UV–vis absorption and transmittance spectra of the IBV/P(HEMA)/$EtMeIm^{+}N(CN)_2^{-}$ /PB device measured under different dc reduction potentials (applied to the blank electrode) in the range of -0.5 to -2.6 V and under oxidation potentials of +0.5 and +1.0 V, are shown in Figure 5. The device encompasses the semi-solid state electrolyte with the ionic liquid: $EtMeIm^{+}N(CN)_2^{-}$ and 25 wt.% of the polymer P(HEMA) and 25 mM IBV salt dissolved therein. A PB film served as the charge balancing

counter electrode layer in the device. Under oxidation potentials of +0.5 V, +1.0 V and in the as-fabricated state, the device shows an absorption peak at 385 nm, which is attributed to the charge transfer between the IBV^{2+} cation and the Br^- anion [33]. No strong absorption is seen in the visible region (Figure 5a). Upon applying a reduction potential of –1.0 V to the device, a blue film of the IBV radical cation (which is insoluble in the electrolyte) is formed on the FTO surface corresponding to the IBV^{2+} to $IBV^{+\bullet}$ transition. The blue color deepens and an absorption peak (λ_{max} at around 605 nm) reflecting the corresponding increase in the number of color centers or the radical cation proportion, progressively gains intensity with increasing potential. This peak is assigned to the intra-molecular charge transfer in the bipyridyl moiety of IBV radical cation. The device attains a deep blue color in the fully reduced state (E = -2.6 V), and a photograph showing the blue device is also shown in Figure 5c. Two satellite peaks at 562 and 664 nm, on either side of the main absorption peak are also observed and these have pronounced intensities in the fully reduced state (E = -1.0 to -2.6 V). Whilst reduction of IBV^{2+} to $IBV^{+\bullet}$ occurs at the cathode, at the anode the Prussian white (PW) oxidizes to form Prussian blue (PB). The two processes are complementary and a dark blue hue is achieved for the device. The reason for the retention of the deep blue hue even at a high cathodic potential of -2.6 V, is the comproportionation reaction, which causes the neutral viologen to react with a di-cation and form the radical cation, as expressed in equation (2) [6]. The spectral peak below 410 nm also experiences an intensity enhancement as the applied reduction potential is raised from -0.5 V to -2.6 V; this could be due to increased interaction between positively charged $IBV^{+\bullet}$ moieties and the negatively charged dicyanamide ions from the electrolyte gel [34]. However, upon further increasing the cathodic potential to values above -2.6 V, air-bubbles were formed in the device, and the absorption intensity acquired saturation. On the other hand, in the fully oxidized state (+1.0 V applied to the blank FTO electrode in the device), the device acquires an almost transparent hue which can also be perceived in the inset of Figure 5c.

In the reduced state, the deposited viologen radical cations are somewhat stabilized as mono- cation radical species on the FTO surface possibly due to the steric hindrance offered by the bulky imidazole groups attached to the bi-pyridinium radical cations, which prevents radical couplings. Evan *et al.* previously observed that mesityl viologens, do not undergo radical dimerization even at low temperatures [35]. But here, the steric crowding engendered by the benzimidazole groups, does not allow the two mono radical cations or $IBV^{+\bullet}$ to approach close enough for the spin-pairing interaction to overcome the repulsion energy. This can be observed in the UV-visible spectra, Figure 5a, as there were no absorptions around 900 nm region, which are generally observed whenever viologen dimers are formed [7,36]. The transmittance versus wavelength plots for the device, under the same reduction/oxidation potentials are displayed in Figure 5b. The bleached state transmittance of the device is 65.5% at 605 nm when an external bias of 0 V was applied. The maximum transmission modulation (ΔT = T (+1.0 V) – T (-2.6 V)) offered by the device, at photopic wavelengths of 500 and 605 nm are 19.4 and 30.5 % respectively, which are sufficient for electrochromic window applications. In the past, Lin et al. observed a transmission modulation of 59% at 609 nm, for a PB and a heptyl viologen ($HV(BF_4)2$) solution based electrochromic device [37].

When a series of voltages (from -1.0 to -2.6 V) are applied, the device gets colored; the values of injection charge were determined at each bias by chronoamperometry and these values were used for plotting the optical density change (ΔOD) versus inserted charge per unit area (Q/A) (Figure 5c). The slope of the ΔOD versus intercalated charge per unit area profile yields the coloration efficiency (CE) of the device at a monochromatic wavelength. We used 605 nm or λ_{max} for calculating the coloration efficiency and the reference potential for estimating the ΔOD values was +1.0 V. Coloration efficiency was therefore deduced the following equation.

$$CE \text{ or } \eta(\lambda) = \Delta OD(\lambda)/Q/A \qquad (3)$$

The coloration efficiency at 605 nm is calculated to be 725 cm^2 C^{-1} for the IBV/P(HEMA)/$EtMeIm^+N(CN)_2^-$/PB device. Our value is substantially higher than the reported values of CE for pristine electrochromic viologens. This could be due to the bulky substituents on the bipyridyl, which make bleaching easier and also due to the high electrochemical activity of the viologen. In a previous report, Hu *et al.* observed a CE of 342.2 cm^2 C^{-1} (at 610 nm) for an all-solid-state electrochromic device with heptyl viologens [13] and in yet another study, a CE of 163 cm^2 C^{-1} (at 650 nm) was observed for a device based on poly(butyl viologen) [3]. A composite of In/Sn oxide nanoparticles and heptyl viologen showed a CE of 912 cm^2 C^{-1}[14].

The color-bleach characteristics for the IBV/P(HEMA)/$EtMeIm^+N(CN)_2^-$/PB device were recorded at half-cycles corresponding to 3.0 s and 5.0 s and by switching potentials of ±2.0 V (Figure 6a). The kinetic responses were recorded at the λ_{max} of 605 nm. Coloration time, defined as the time required for the device to acquire a 90 % of the total absorption change was observed to be 2.1 and 2.5 s (when subjected to step times of 3 and 5 s respectively). Bleaching time, defined as the time taken by the device to undergo a 90 % decrease (of the complete absorption change) was 2.2 and 3.3 s for 3 and 5 s half-cycles. Our color-bleach times are comparable to values of 1.3 and 4.7 s reported for viologen based devices [3,13]. The device was subjected to continuous cycling at a scan rate of 100 mV s^{-1}, between –0.8 to +0.2 V and the CV plots for the first and thousandth cycle are displayed in Figure 6b. The cathodic peak current decreased only by 18.9 % of its original value after 1000 cycles, indicating that the IBV salt based device can endure repetitive transparent ↔ blue transitions without undergoing degradation. Such a robust, high contrast device is most conducive for electrochromic window applications.

3.5 Electrochemical impedance spectroscopy

To understand how transmission modulation and coloration efficiency are controlled by the internal circuit elements in the device, EIS spectra of the IBV/P(HEMA)/$EtMeIm^+N(CN)_2^-$/PB device were

recorded by superimposition of voltage of 10 mV over different magnitudes of dc potentials. All potentials were applied to the blank FTO electrode of the device. The equivalent circuit displayed in the inset of Figure 7 was found to give excellent fits almost over the entire frequency range of 1 MHz to 0.1 Hz under consideration. The Z″ *versus* Z′ curve for the device, under all dc potentials shows an inclined line profile, except for the curve at -2.0 V, which comprises of a semicircle followed by the straight line response. The point of commencement of the Z″ versus Z′ curve, corresponds to the bulk resistance of the ionic liquid based solid polymer electrolyte which lies in the range of ~50 – 60 Ω (over different applied potentials), and its' value was largely independent of the applied dc bias. The subsequent curvature is explained by a parallel combination of resistance due to charge transfer (R_{CT}) at the IBV^{2+} gel/FTO interface and the corresponding electrical double layer capacitance (C_{dl}). The magnitude of R_{CT} increases (from 7.7 μΩ to 26.0 μΩ) with increasing reduction potentials, i.e. ongoing from -0.5 to -1.0 V and in this range, the profile is quasi-linear. The curve tilts towards the real (resistive component, Z′) axis, at -2.0 V and the R_{CT} has a value of 35.3 Ω while C_{dl} decreases from 34 to 18 μF (ongoing from -0.5 to -2.0 V). The magnitude of charge transfer resistance is a measure of the ease with which ions are transferred across the electrode/electrolyte interface; and here the value of R_{CT} is extremely low under low reduction potentials of -0.5 to -1.0 V, it varies between 7.7 to 26 μΩ; coloration in this potential range is therefore induced by a capacitive Faradaic charging mechanism rather than resistive charge transfer. However, once the insoluble radical cation ($IBV^{+\bullet}$) forms a blue layer over the FTO surface, further insertion of electrons from the external circuit and release of anions from the viologen backbone into the gel electrolyte are hindered by the bulk of this film and therefore the profile acquires a dominant resistive component than capacitive. On subjecting this electrode to potentials of +0.5 and +1.0 V, the curve again reverts to a capacitive response, primarily because the $IBV^{+\bullet}$ film dissolves in the gel by undergoing oxidation to the IBV^{2+} di-cation, and therefore only the double layer of charge encompassing the negatively charges from the dicyanamide and bromide anions in the gel and the

positive charges on FTO surface contributes to impedance. It is apparent that both the resistive and capacitive charging- charge transfer mechanisms operative at negative potentials, commensurate with the high optical density change achieved for the device which effectively translates into a high coloration efficiency of 725 cm^2 C^{-1}.

Conclusions

A novel 1,1′-bis[4-(5,6-dimethyl-1*H*-benzimidazole-1-yl)butyl]-4,4′-bipyridinium dibromide (viologen) (IBV) was synthesized and characterized. XPS studies ascertained the formation of the IBV salt as distinctive contributions from quaternary and neutral nitrogens and electrostatically bonded bromide were obtained. The viologen was incorporated in an electrochromic device, by dissolution in a dicyanamide based ionic liquid-gel electrolyte having large ionic conductivity, good thermal stability upto 200 ^oC and wide electrochemical potential stability window (of ~4 V) and moderately high optical transparency in the visible region. The device exhibited reversible switching between colorless and dark blue states, which commensurate with high transmission modulation of 30.5 % at 605 nm, an outstanding coloration efficiency of 725 cm^2 C^{-1} (at 605 nm), good color homogeneity and rapid response times of 2-3 s. The high electrochemical activity of the IBV (viologen) salt was retained even after 1000 repeated switches between the transparent and colored states. The excellent performance attributes of the electrochromic device with this new viologen/novel ionic liquid based gel electrolyte opens up avenues to develop variants of dimethylbenzimidazole based derivatives of 4,4′-bipyridyl, for application in both transmissive and reflective electrochromic devices.

Supporting Information Available

^1H and ^{13}C NMR spectra for the compound (**2**) and ^1H NMR spectrum of (**3**).

Acknowledgements

Financial support from Department of Science & Technology (DST/TSG/PT/2007/69) is gratefully acknowledged. One of the authors, Rambabu Sydam acknowledges University Grants Commission for junior research fellowship.

References

[1] P.M.S. Monk, R.J. Mortimer, D.R. Rosseinsky, Electrochromism and Electrochromic Devices, Cambridge University Press, Cambridge, UK, 2007.

[2] D.R. Rosseinsky, R.J. Mortimer, Adv. Mater. 13 (2001) 783.

[3] T. -H. Kuo, C.-Y. Hsu, K. -M. Lee, K. -C. Ho, Solar Energy Mater. Solar Cells 93 (2009) 1755.

[4] R. Cinnsealach, G. Boschloo, S.N. Rao, D. Fitzmaurice, Solar Energy Mater. Solar Cells 55 (1998) 215.

[5] R.J. Mortimer, Chem. Soc. Rev. 26 (1997) 147.

[6] P.M.S. Monk, The Viologens: Physicochemical Properties, Synthesis and Applications of the Salts of 4,4′-Bipyridine, J. Wiley & Sons: Chichester, U.K., 1998.

[7] R.J. Mortimer, Electrochim. Acta 44 (1999) 2971.

[8] H.J. Kim, J.K. Seo, Y.J. Kim, H.K. Jeong, G.I. Lim, Y.S. Choi, W.I. Lee, Solar Energy Mater. Solar Cells 93 (2009) 2108.

[9] G. Wang, X. Fu, J. Huang, C. Wu, L. Wu, Q. Du, Org. Elec. 12 (2011) 1216.

[10] R.J. Mortimer, T.S. Varley, Chem. Mater. 23 (2011) 4077.

[11] S.Y. Choi, M. Mamak, N. Coombs, N. Chopra, G. A. Ozin, Nano Lett. 4 (2004) 1231.

[12] V. Jain, M. Khiterer, R. Montazami, H.M. Yochum, K.J. Shea, J.R. Heflin, Appl. Mater. Interfaces 1 (2009) 83.

[13] C.-W. Hu, K.-M. Lee, K.-C. Chen, L. -C. Chang, K.-Y. Shen, S.-C. Lai, T. -H. Kuo, C.-Y. Hsu, L. -M. Huang, R. Vittal, K.-C. Ho, Solar Energy Materials & Solar Cells 99 (2012) 135.

[14] Y. Rong, S. Kim, F. Su, D. Myers, M. Taya, Electrochim. Acta 56 (2011) 6230.

[15] D.M. De Longchamp, M. Kastantin, P.T. Hammond, Chem. Mater. 15 (2003) 1575.

[16] R.J. Mortimer, A. L. Dyer, J.R. Reynolds, Displays 27 (2006) 2.

[17] H.J. Byker, Bipyridinium salt solutions, *US Patent* 5,294,376, 1994.

[18] H.J. Byker, Electrochromic devices with bipyridinium salt solutions, US Patent 5,336,448, 1994.

[19] P.R. Somani, S. Radhakrishnan, Mater. Chem. Phys. 77 (2002) 117.

[20] C.L. Bird, A.T. Kuhn, Chem. Soc. Rev. 10 (1981) 49.

[21] H.T. Van Dam, J.J. Ponjee, J. Electrochem. Soc. 121 (1974) 1555.

[22] M. Deepa, A. Awadhia, S. Bhandari, Phys. Chem. Chem. Phys. 11 (2009) 5674.

[23] S. Bhandari, M. Deepa, S. Pahal, A.G. Joshi, A.K. Srivastava, R. Kant, ChemSusChem 3 (2010) 97.

[24] R.Sydam, M. Deepa, A.K. Srivastava, RSC Adv. 2 (2012) 9011.

[25] I. Mazov, D. Krasnikov, A. Stadnichenko, V. Kuznetsov, A. Romanenko, O. Anikeeva, E. Tkachev, J. Nanotech. 2012 (2012) 1.

[26] Z. Jian, H.-T. Liu, B. Wu, C.-A. Di, Y.-L. Guo, T. Wu, G. Yu, Y.-Q. Liu, D.-B. Zhu, Sci Rep. 2 (2012) 662.

[27] Y.P. Zhang, J.H. He, G.Q. Xu, J. Phys. Chem. C 116 (2012) 8943.

[28] J. Reiter, O. Krejza, M. Sedlarkova, Solar Energy Mater. Solar Cells 93 **(**2009) 249.

[29] D.R. Rosseinsky, P.M.S. Monk, J. Chem. Soc. Faraday Trans. 89 (1993) 219.

[30] D.R. Rosseinsky, P.M.S. Monk, J. Chem. Soc. Faraday Trans. 86 **(**1990) 3597.

[31] G. Chidichimo, M.D. Benedittis, J. Lanzo, B.C.D. Simone, D. Imbardelli, B. Gabriele, L. Veltri, G. Salerno, Chem. Mater. 19 (2007) 353.

[32] A.F. Sammells, N.U. Pujare, J. Electrochem. Soc.133 (1986) 1270.

[33] R.J. Mortimer, T.S. Varley, Solar Energy Mater. Solar Cells 99 (2012) 213.

[34] P. Cea, S. Martin, A. Villares, D. Mobius, M.C. Lopez, J. Phys. Chem. B 110 (2006) 963.

[35] J.C. Evans, C.C. Rowlands, C.R. Morris, J. Chem. Soc. Perkin Trans. II 9 (1987) 1375.

[36] P.M.S. Monk, R.D. Fairweather, J. A. Duffy, M.D. Ingram, J. Chem. Soc. Perkin Trans. II (1992) 2039.

[37] C.-F. Lin, C.-Y. Hsu, H.-C. Lo, C.-L. Lin, L.-C. Chen, K.-C. Ho, Solar Energy Mater. Solar Cells 95 (2011) 3074.

Figure Captions

Figure 1 (a) XPS survey spectrum, and deconvoluted core level spectra of (b) C1s and (c) N1s and (d) Br3d of IBV salt. Inset of (d) shows the enlarged view of the Br3p peak from IBV salt.

Figure 2 (a) TGA curves for the pristine ionic liquid: [$EtMeIm^+N(CN)_2^-$] (○) and the P(HEMA)/$EtMeIm^+N(CN)_2^-$/DMF gel electrolyte (□), (b) LSV plot of the P(HEMA)/$EtMeIm^+N(CN)_2^-$/DMF gel electrolyte recorded at a scan rate of 20 mV s^{-1} between two Pt electrodes, (c) variation of transmittance as a function of wavelength and (d) ionic conductivity *versus* reciprocal absolute temperature curve for the P(HEMA)/$EtMeIm^+N(CN)_2^-$/DMF gel electrolyte. Inset of (c) shows a photograph of the semi-solid gel.

Figure 3 TGA plot of the IBV salt in the 30 – 600 ^oC temperature range. Digital photographs of the as-synthesized yellow colored IBV salt, and solutions of (a) blank electrolyte: HEMA-DMF-IL (b) IBV salt in electrolyte and (c) IBV salt dissolved in a solution of sodium hydrosulfite in ammonia, showing the chemical reduction of IBV^{2+} to $IBV^{+\bullet}$ (blue).

Figure 4 Cyclic voltammograms of the IBV/P(HEMA)/$EtMeIm^+N(CN)_2^-$/PB device recorded between potential limits of (a) –0.8 and +0.2 V and (b) –1.5 and +0.2 V at a scan rate of 2 mV s^{-1} and (c) between–0.8 and +0.2 V at different scan rates of 2, 5, 10, 20, 50 and 100 mV s^{-1}.

Figure 5 *In-situ* (a) absorption spectra and (b) normalized transmission spectra of the IBV/P(HEMA)/EtMeIm$^+$N(CN)$_2^-$/PB device recorded under different reduction potentials of: –0.5 V and from –1 to –2.6 V in steps of 0.2 V, and under oxidation potentials of +0.5 and +1.0 V; all potentials applied to the blank FTO electrode or cathode of the device. (c) *ΔOD versus* charge density plot at a monochromatic wavelength of 605 nm (•) for the IBV/P(HEMA)/EtMeIm$^+$N(CN)$_2^-$/PB device with OD response under +1 V in (a) used as reference for determination of *ΔOD*. Digital photographs of the electrochromic device in fully colored (E = –2.6 V) and fully bleached (E = +1.0 V) states are shown as an inset of (c).

Figure 6 (a) Normalized absorbance *versus* time curves for the IBV/P(HEMA)/EtMeIm$^+$N(CN)$_2^-$/PB device at a λ_{max} of 605 nm, under a square wave dc potential of ±2.0 V and under step times of 3 (—) and 5 (…..) s. (b) Cyclic voltammograms of the IBV/P(HEMA)/EtMeIm$^+$N(CN)$_2^-$/PB device recorded in the 1st cycle (—) and after 1000 cycles (----) (scan rate = 100 mV s^{-1}).

Figure 7 Electrochemical impedance spectra of the IBV/P(HEMA)/EtMeIm$^+$N(CN)$_2^-$/PB device recorded under dc potentials of: 0 (△), +0.5 (○), +1.0 (☆) V and −0.5 (◇), −1 (✳), −1.5 (▽) and −2.0 (□) V, over a frequency range of 0.1 to 10^6 Hz; dc potential applied to the blank FTO electrode/cathode. Inset shows the equivalent circuit used for fitting the experimental data.